

## A Nuclear Many-Body Theory at Finite Temperature Applied to Protoneutron Star.

GUILHERME F. MARRANGHELLO\*, CESAR A. Z. VASCONCELLOS  
*Instituto de Física, Universidade Federal do Rio Grande do Sul  
91501-970 Porto Alegre - RS, Brasil*

MANFRED DILLIG  
*Institut für Theoretische Physik III, der Universität Erlangen-Nürnberg  
D-91058 Erlangen, Germany*

and

J. A. DE FREITAS PACHECO  
*Observatoire de la Côte d'Azur  
Nice, France*

Received (received date)  
Revised (revised date)

### Abstract

Thermodynamical properties of nuclear matter are studied in the framework of an effective many-body field theory at finite temperature, considering the Sommerfeld approximation. We perform the calculations by using the nonlinear Boguta and Bodmer model, extended by the inclusion of the fundamental baryon octet and leptonic degrees of freedom. Trapped neutrinos are also included in order to describe protoneutron star properties through the integration of the Tolman-Oppenheimer-Volkoff equations, from which we obtain, beyond the standard relations for the masses and radii of protoneutron stars as functions of the central density, new results of these quantities as functions of temperature. Our predictions include: the determination of an absolute value for the limiting mass of protoneutron stars; new structural aspects on the nuclear matter phase transition via the behaviour of the specific heat and, through the inclusion of quark degrees of freedom, the properties of a hadron-quark phase transition and hybrid protoneutron stars.

Keywords: Quantum-Hydrodynamics, Finite Temperature, Protoneutron Star

### 1. Introduction

In the last few decades, studies on the evolution of compact stars became a central issue related to theoretical and experimental research on the equation of

---

\*E-mail: gfm@if.ufrgs.br

state (EOS) of dense matter. In 1967, the first pulsar was observed<sup>1</sup> and, based on characteristic observational features, this object was identified as a rotating neutron star. Since this direct evidence for the existence of neutron stars, nuclear models have been widely employed in the description of the internal structure, composition, dynamics and evolution of these massive compact stars. As under the pull of gravity, the energy density in the core of compact stars is thought to approach or even exceed the critical value of  $1 \text{ GeV}/\text{fm}^3$ , i.e. more than 6 times the density of nuclear matter, their structure depends sensitively on the equation of state for very dense matter. As the

EOS describes how the energy density and pressure vary with density and temperature,

it should be also able to describe different phases, including gaseous nuclear matter and liquid nuclei structure up to the deconfinement transition.

The EOS provided by model calculations and the Tolman-Oppenheimer-Volkoff (TOV) equations<sup>2,3</sup> characterize the structure of the star, whose properties like mass, radius, crust extent, moment of inertia are then susceptible to be compared to observations<sup>4</sup>. Moreover, these models should also provide the description of relevant dynamical properties of compact stars as the rotational period, the emission of neutrinos and gravitational waves as well as more fundamental aspects involving the evolution, internal composition and structure of these stellar objects.

Concerning neutron stars, nuclear matter models should be able to account for such objects at least as massive as the most massive observed pulsar, representing an important constraint on any proposed EOS for dense matter. Presently, the best mass determination corresponds to the binary pulsar PSR 1913+16 ( $M = 1.444M_{\odot}$ ). Other estimates based on quasi-periodic oscillations (QPOs), observed in the X-ray emission of low mass binaries (LMXBs) suggest values up to  $2.0 - 2.2M_{\odot}$ , but these results are quite uncertain since they are model-dependent. More recently, from new radial velocity data, the mass of the neutron star associated to the X-ray source in the system Vela X-1<sup>5</sup> was recalculated with a larger accuracy than precedent estimates: the resulting value is  $1.86 \pm 0.16M_{\odot}$ . For a given family of stars, stiffer EOS predict higher limiting mass and larger radii ( $R > 10 - 12 \text{ km}$ ). In particular, recent hydrodynamics models point to EOS stiffer than those expected on the basis of a non-relativistic approach, in better agreement with Vela X-1 results.

In the theoretical treatment of properties of compact stars, the relativistic phenomenological approach developed by Walecka<sup>6</sup>, quantum hadrodynamics (QHD), represents one of the most important approaches to the highly nonlinear behavior of QCD at the hadronic energy scales. QHD model is a relativistic quantum field theory based on a local lagrangian density which uses the nucleon and two meson fields, the scalar-isoscalar, attractive  $\sigma$  and the vector-isoscalar, repulsive  $\omega$ , as the relevant effective degrees of freedom. This model provides a thermodynamically consistent theoretical framework for the description of bulk static properties of strong interacting many-body nuclear systems under extreme conditions. The nonlinear model of Boguta and Bodmer (BB)<sup>7</sup> was developed to improve the description of static properties of nuclear matter, relative to the original Walecka model. With the introduction of cubic and quartic scalar meson self-interactions in the lagrangian density, the model has two additional parameters which allow and provide sufficient flexibility to reproduce at saturation density, currently accepted values for the compression modulus of symmetric nuclear matter and the nucleon effective mass.

In this work we investigate static properties of nuclear matter at the high density domain by using a description based on the BB model. As in its original form, the model is not yet suitable for an extrapolation to higher densities, we considerably extend it by considering, at finite temperature, the fundamental baryon octet, lepton degrees of freedom and trapped neutrinos in a consistent way, i.e. through the inclusion of the  $\varrho$ -meson and the additional consideration of the equations for chem-

ical equilibrium and charge neutrality. In section 3 we exceed the limit of hadron degrees of freedom by including quarks and gluons in order to allow a possible transition to quark matter. Within this objective, we focus on a particular process in the evolution of compact stars, preceding the supernova explosion: the formation of a hot collapsed core or a *protoneutron star*<sup>8</sup>, which can reach temperatures as high as few tens of MeV. These hot and dense relativistic objects are formed in a type-II supernova explosion and evolves to a cold neutron star, basically through neutrino emission. Here, this very dense and hot core is able to trap neutrinos, imparting momentum to the outer layers and then cooling as it reaches a quasi-equilibrium state.

Hitherto, practically all microscopic investigations of stars have been performed for dense, cold matter in its ground state. In this work, the evolution of protoneutron stars is studied, extending previous investigations to non vanishing temperatures. The main novel feature of the present study is the formulation of the dynamical equations in the relativistic framework using a mean-field approach. Global static properties as masses and radii are then computed as a function of central densities and temperatures.

## 2. Nuclear Matter

Nowadays, astrophysical observations of compact stars and terrestrial nuclear physics experiments are working together in the determination of the equation of state for dense matter. This allows to test the predictions and consistency of different models for the properties of nuclear matter under extreme conditions, through the comparison of both astrophysical data and results from high energy heavy ion collisions, where nuclear matter approaches similar conditions of density and temperature as in the interior of dense compact stellar objects as neutron and protoneutron stars. Conversely, experiments with relativistic heavy ions at current facilities are now providing first empirical information on the equation of state at high baryon matter densities, particularly relevant to compact stars. Moreover, one feature is of particular interest: in addition to the deconfinement regime at very high densities and temperatures up to  $T_c = 150 \text{ MeV}$  and beyond, there is another phase transition in nuclear matter at much lower excitation energies, analogous to the liquid-gas transition in condensed matter physics. This transition is predicted to occur with temperatures at  $T_c > 15 \text{ MeV}$  and hence is of particular interest for the physics of supernova explosions, and in the formation of protoneutron stars. Intermediate energy heavy ion collisions, at energies around 100 MeV per nucleon, are currently the most promising tools in searching for the liquid-gas transition in laboratory.

The lagrangian density of our approach, which takes into account the fundamental baryon octet, meson sectors, and includes lepton degrees of freedom, is given by

$$\begin{aligned}
\mathcal{L} = & \sum_B \bar{\psi}_B [(i\gamma_\mu(\partial^\mu - g_{\omega B}\omega^\mu) - (M_B - g_{\sigma B}\sigma)]\psi_B \\
& - \sum_B \bar{\psi}_B [\frac{1}{2}g_{\rho B}\boldsymbol{\tau} \cdot \boldsymbol{\rho}^\mu]\psi_B + \frac{bM}{3}\sigma^3 + \frac{c}{4}\sigma^4 \\
& + \frac{1}{2}(\partial_\mu\sigma\partial^\mu\sigma - m_\sigma^2\sigma^2) - \frac{1}{4}\omega_{\mu\nu}\omega^{\mu\nu} + \frac{1}{2}m_\omega^2\omega_\mu\omega^\mu \\
& - \frac{1}{4}\boldsymbol{\rho}_{\mu\nu} \cdot \boldsymbol{\rho}^{\mu\nu} + \frac{1}{2}m_\rho^2\boldsymbol{\rho}_\mu \cdot \boldsymbol{\rho}^\mu + \sum_l \bar{\psi}_l [i\gamma_\mu\partial^\mu - M_l]\psi_l . \quad (1)
\end{aligned}$$

This lagrangian density describes a system of eight baryons ( $B = p, n, \Lambda, \Sigma^-, \Sigma^0, \Sigma^+, \Xi^-, \Xi^0$ ) coupled to three mesons ( $\sigma, \omega, \rho$ ) and leptons. The scalar and vector

coupling constants in the theory,  $g_\sigma$  and  $g_\omega$ , and the coefficients  $b$  and  $c$  for the nonlinear  $\sigma$  self-couplings are determined to reproduce, at saturation density  $\rho_0 = 0.153 \text{ fm}^{-3}$ , the binding energy,  $B = -16.3 \text{ MeV}$ , and the compression modulus,  $K = 240 \text{ MeV}$  of nuclear matter, and the nucleon effective mass,  $M^* = 732 \text{ MeV}$ . Additionally, the isovector coupling constant  $g_\rho$  is determined from the symmetry energy coefficient,  $a_4 = 32.5 \text{ MeV}$ , in nuclear matter. The hyperon/nucleon coupling constant ratios  $\chi_i = g_{Hi}/g_i$ , with  $i = \sigma, \omega$ , are constrained through the binding energy of the  $\Lambda$ -hyperon in nuclear matter, from hypernuclear spectroscopy and the lower bound of the mass of a neutron star; altogether they determine the ratios of the hyperon/nucleon coupling constants, which correlate the relative strengths of the  $\sigma$  and  $\omega$  mean-fields to the nucleon and hyperons:

$$(B/A) = \chi_\omega V - \chi_\sigma S, \quad (2)$$

and where  $V = (g_\omega/m_\omega)^2 \rho_0$  and  $S = (M - M^*)$  are the mean-field vector and scalar potentials, respectively.

To determine the nuclear matter equation of state at finite temperature we use a set of model parameterizations known as GM3<sup>9</sup>. With this set of parameters, we find for the nucleon effective mass, at saturation density and for the compression modulus of nuclear matter, results in the range of current experimental values for these quantities as for instance the above cited ones. The effects of nonlinear scalar self-couplings are studied by Koepf et. al.<sup>10</sup>. Though the ratios  $\chi_i$  are known only qualitatively, studies have shown however that QHD predictions of bulk static properties of neutron stars<sup>4</sup> are very sensitive to different choices for  $\chi_i$ .

Neutrinos, which are not included in the original approach for the GM3 parameters, are an indispensable agency for protoneutron star studies. Neutrinos are thus included in our formulation, at chemical equilibrium, via the lepton fraction ratio

$$Y_L = \frac{\rho_e + \rho_\nu}{\rho_B}, \quad (3)$$

where  $\rho_e$ ,  $\rho_\nu$  and  $\rho_B$  represent, respectively, the electron, neutrino and baryon densities. Explicitly, we extract the lepton fraction  $Y_L$  from the study of the gravitational collapse of the core.

The values for the scalar ( $\sigma$ ), vector ( $\omega$ ) and isovector ( $\rho$ ) GM3 coupling constants,  $(g_i/m_i)^2$ , with  $i = \sigma, \omega, \rho$ , are shown in table 1 together with the hyperon/nucleon coupling constant ratios, and the lepton fraction,  $Y_L$ .

Table 1: Parameters adopted in the model.

$(g_\sigma/m_\sigma)^2$ $\text{fm}^2$	$(g_\omega/m_\omega)^2$ $\text{fm}^2$	$(g_\rho/m_\rho)^2$ $\text{fm}^2$	b ( $\times 100$ )	c ( $\times 100$ )
9.927	4.820	4.791	0.8659	-0.2421
$\chi_\sigma$	$\chi_\omega$	$\chi_\rho$	$Y_L$	-
0.6	0.568	1.0	0.4	-

Applying standard technics from field theory and the mean-field approach, we obtain the equation of state for nuclear matter as a parametric equation  $p = p(\epsilon)$  which explicitly relates the energy density

$$\epsilon = \frac{1}{2}m_\sigma^2\sigma^2 + \frac{1}{2}m_\omega^2\omega_0^2 + \frac{1}{2}m_\rho^2\rho_{03}^2 + \frac{bM}{3}\sigma^3 + \frac{c}{4}\sigma^4$$

$$\begin{aligned}
 & + \sum_B \frac{2J_B + 1}{(2\pi)^3} \int_0^\infty \sqrt{k^2 + M_B^{*2}} [n(\mu_B, T) + \bar{n}(\mu_B, T)] d^3k \\
 & + \sum_\lambda \frac{2}{(2\pi)^3} \int_0^\infty \sqrt{k^2 + m_\lambda^2} [n(\mu_\lambda, T) + \bar{n}(\mu_\lambda, T)] d^3k, \quad (4)
 \end{aligned}$$

and pressure

$$\begin{aligned}
 p = & -\frac{1}{2}m_\sigma^2\sigma^2 + \frac{1}{2}m_\omega^2\omega_0^2 + \frac{1}{2}m_\rho^2\rho_0^2 + \frac{bM}{3}\sigma^3 + \frac{c}{4}\sigma^4 \\
 & + \frac{1}{3} \sum_B \frac{2J_B + 1}{(2\pi)^3} \int_0^\infty \frac{k^2}{\sqrt{k^2 + M_B^{*2}}} [n(\mu_B, T) + \bar{n}(\mu_B, T)] d^3k \\
 & + \frac{1}{3} \sum_\lambda \frac{2}{(2\pi)^3} \int_0^\infty \frac{k^2}{\sqrt{k^2 + m_\lambda^2}} [n(\mu_\lambda, T) + \bar{n}(\mu_\lambda, T)] d^3k. \quad (5)
 \end{aligned}$$

In the expressions above we may identify, in the first row of both, the contributions of the scalar, vector and isovector mesons, followed by the contributions of the Fermi gas of baryons and leptons; these contributions appear as sums over the particle families,  $B = n, p, \Sigma, \Xi, \Lambda$  and  $\lambda = e, \mu, \nu$ , and where  $J_B$  is the isospin baryon number. The quantities  $n(\mu, T)$  and  $\bar{n}(\mu, T)$  are the Fermi-Dirac distribution functions for particle and anti-particles, at finite temperature:

$$\begin{aligned}
 n(\mu_B, T) & = [e^{\beta(\sqrt{\kappa^2 + M_B^{*2}} - \mu_B + \frac{g_\omega}{m_\omega^2}\rho_B + \frac{g_\rho}{m_\rho^2}\rho_3)} + 1]^{-1}, \\
 \bar{n}(\mu_B, T) & = [e^{\beta(\sqrt{\kappa^2 + M_B^{*2}} + \mu_B - \frac{g_\omega}{m_\omega^2}\rho_B - \frac{g_\rho}{m_\rho^2}\rho_3)} + 1]^{-1}, \quad (6)
 \end{aligned}$$

with  $\beta = 1/\kappa T$  and the chemical potentials  $\mu_B$  and  $\mu_\lambda$  for baryons and leptons, respectively (see Figs.1 and 2 where the Fermi distribution function and the density of states are plotted as functions of chemical potential and the squared momentum  $\varepsilon$ , respectively).

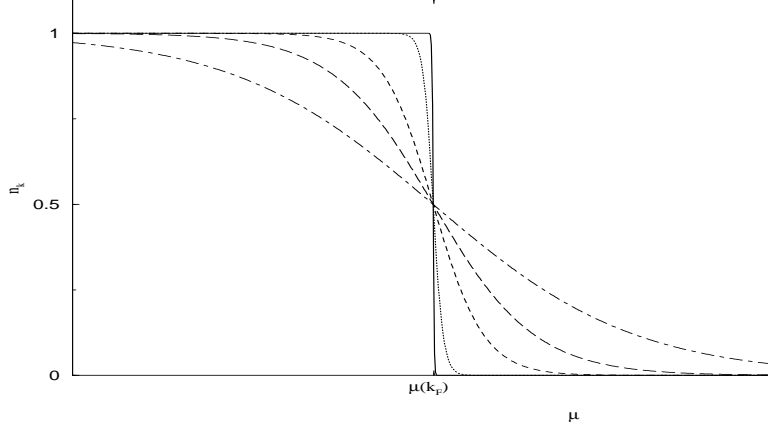


Figure 1: Fermi distribution  $n_k$  as a function of the baryon chemical potential for  $T=0\text{MeV}$  (solid line),  $T=10\text{MeV}$  (dotted line),  $T=50\text{MeV}$  (dashed line),  $T=100\text{MeV}$  (long dashed line) and  $T=200\text{MeV}$  (dot-dashed line).

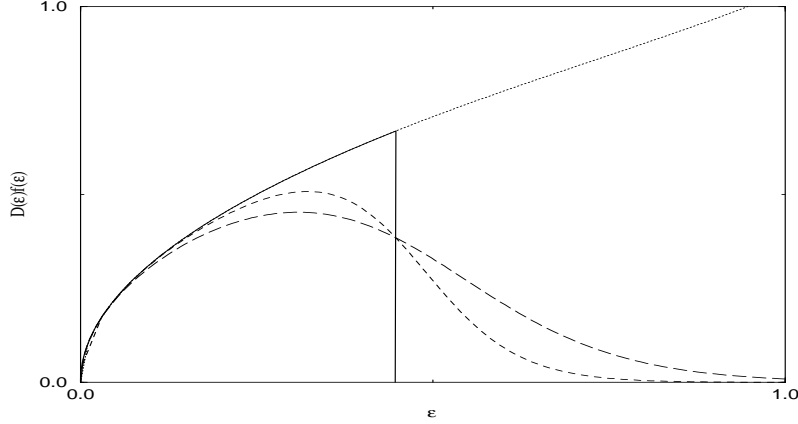


Figure 2: Density of states as a function of baryon squared momentum for  $T=0\text{MeV}$  (solid line),  $T=50\text{MeV}$  and  $T=100\text{MeV}$

In the numerical calculations with the BB model, we have considered hyperonic matter without (Fig.3) and with trapped neutrinos (Fig.4), and at a higher temperature ( $T=50\text{MeV}$  in Fig.5) in order to evaluate the effect of these quantities on proton-neutron star properties.

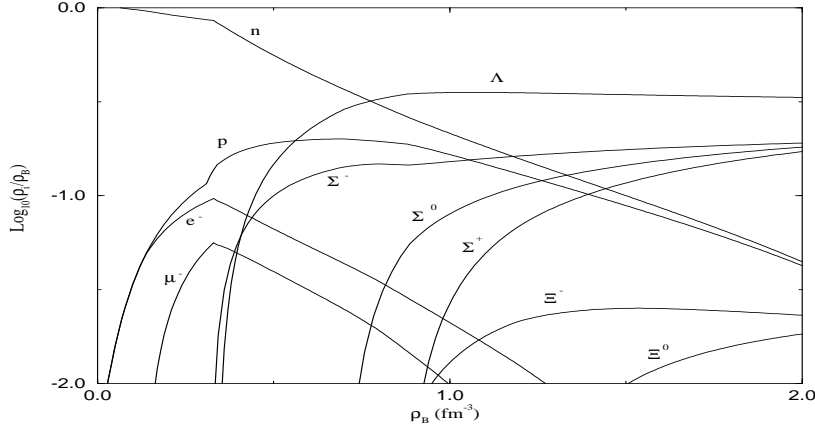


Figure 3: Distribution of particles as a function of baryon density for  $T=10\text{MeV}$ , without neutrino degrees of freedom.

A liquid-gas phase transition is predicted in various relativistic nuclear models such as QHD, BB and others, when symmetric nuclear matter or pure neutron matter are described. However, following within the same models to describe asymmetric nuclear matter, via the inclusion of the  $\rho$ -meson, this phase transition disappears. Instead, the energy used to generate this liquid-gas phase transition, leads now to hyperon production, resulting in a phase transition of asymmetric nuclear matter into hyperonic matter. In such a phase transition, the system has to provide an extra energy to convert nucleons into hyperons which makes the corresponding EOS stiffer. The provision of this extra energy is not easily seen in this case in the EOS (Fig.6), as it is in the former Van der Waals liquid-gas phase transition. It is however clearly visible in the curve for the specific heat, where each hyperon generation formed introduces a discontinuity on its structure (Fig.7). This phase

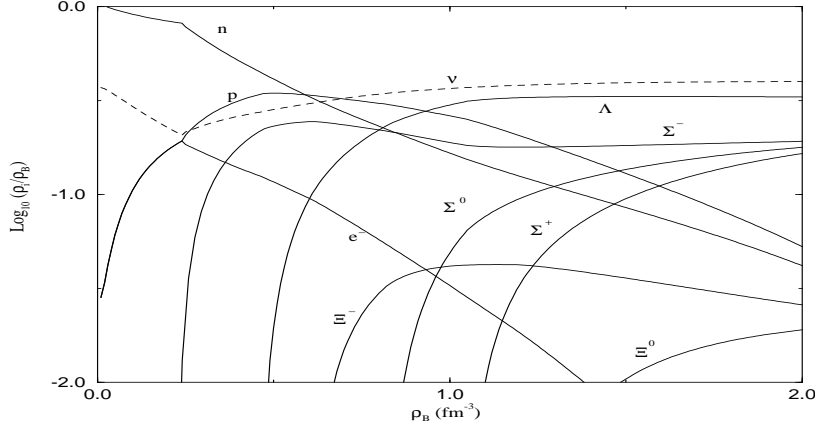
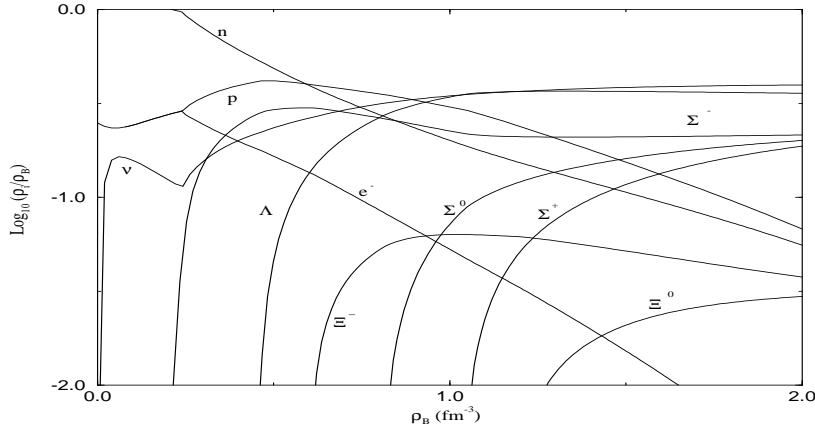


Figure 4: As figure 3, including however neutrinos in the calculations.


Figure 5: As figure 4, however for  $T=50\text{MeV}$ .

transition is similar to the corresponding one with the formation of Cooper pairs in the superconductivity phenomena in electron systems, where discontinuities are also found instead of singularities, characterizing this type of behaviour as a continuous phase transition.

### 3. Quark Matter

We have developed so far, nuclear matter studies disregarding the presence of quarks and gluons degrees of freedom. However, the extreme conditions for the density in the interior of a protoneutron star may be favorable for the occurrence of a hadron-quark phase transition, which may form a core of a quark-gluon plasma (QGP) in the inner regions of the star.

We make use of the MIT bag model<sup>11</sup> in order to describe the quark matter equation of state and the hadron-quark phase transition. The MIT lagrangian is given as

$$\mathcal{L}_{MIT} = \left[ \frac{i}{2} (\bar{\psi} \gamma^\mu \partial_\mu \psi - (\partial_\mu \bar{\psi}) \gamma^\mu \psi) - B \right] \Theta_V(x) - \frac{1}{2} \bar{\psi} \psi \Delta_s, \quad (7)$$

(for details on the meaning of the symbols, see for instance<sup>12</sup>). Following again stan-

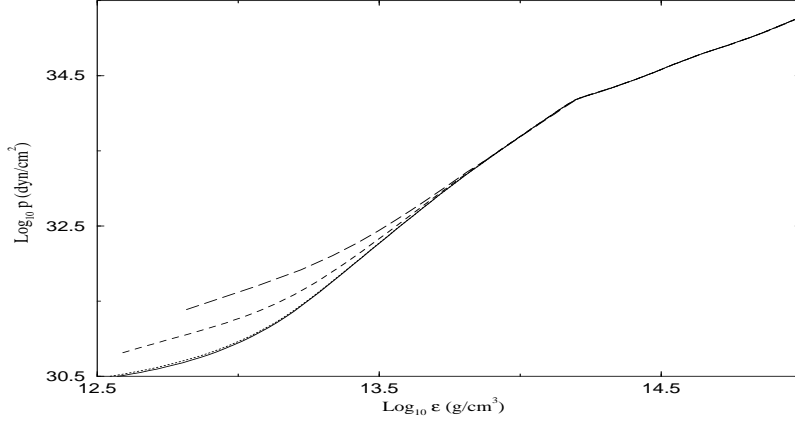


Figure 6: Nuclear matter equation of state for  $T=0\text{MeV}$  (solid line),  $T=50\text{MeV}$  (dotted line) and  $T=100\text{MeV}$  (dashed line).

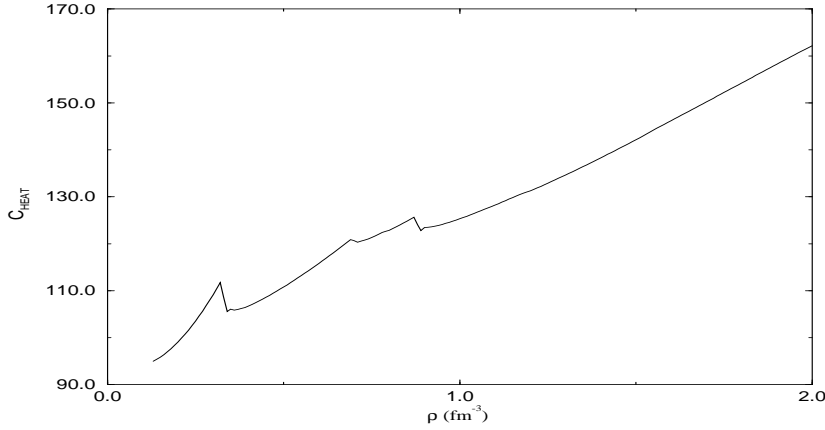


Figure 7: Specific heat as a function of baryon density for  $T=10\text{MeV}$ .

standard technical procedures of quantum field theory, this lagrangian density generates the following equation of state for quark matter ( $p = p(\epsilon)$ ):

$$\epsilon = B + \sum_f \frac{\gamma_f}{2\pi^2} \int_0^\infty k^3 dk [n_k(\mu) + \bar{n}_k(\mu)], \quad (8)$$

$$p = -B + \sum_f \frac{1}{3} \frac{\gamma_f}{2\pi^2} \int_0^\infty k^3 dk [n_k(\mu) + \bar{n}_k(\mu)], \quad (9)$$

with the degeneracy factor represented by  $\gamma_f = 2_{spin} \times 3_{colour}$  and the bag constant denoted by  $B$ . The baryon density is given by

$$\rho_B = \sum_f \frac{1}{3} \frac{\gamma_f}{2\pi^2} \int_0^\infty k^2 dk [n_k(\mu) - \bar{n}_k(\mu)]. \quad (10)$$



The hadron-quark phase transition is determined via the Gibbs criteria<sup>13</sup>, which require that, at constant temperature, pressure and chemical potential of both hadron (H) and quark (Q) phases are related by

$$\begin{aligned} P_Q &= P_H, \\ \mu_Q &= \mu_H, \end{aligned} \quad (11)$$

for a conserved overall baryon number, i.e.

$$N_Q/3 + N_H = \text{constant}, \quad (12)$$

where  $N_Q$  is the number of quarks and  $N_H$  is the number of baryons in the system.

The resulting equation of state includes the presence of hadrons, with a phase of deconfined quark matter represented in Fig.8, and where the plateau shown in the figure reflect the Gibbs condition of the phase transition.

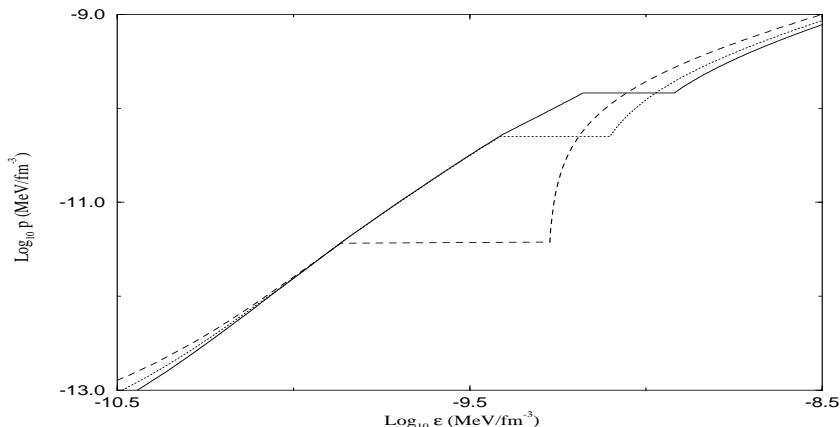


Figure 8: Equation of state with the hadron-quark phase transition for a bag constant  $B = 100 \text{ MeV}/\text{fm}^3$  (solid line),  $B = 131.2 \text{ MeV}/\text{fm}^3$  (dotted line) and  $B = 150 \text{ MeV}/\text{fm}^3$  (dashed line).

#### 4. Stellar Structure

The protoneutron star configuration may be determined by combining the nuclear matter EOS with the TOV equations from general relativity:

$$4\pi r^2 dp(r) = -\frac{M(r)dm(r)}{r^2} \left(1 + \frac{p(r)}{\epsilon(r)}\right) \left(1 + \frac{4\pi r^3 p(r)}{M(r)}\right) \left(1 - \frac{2M(r)}{r}\right)^{-1}, \quad (13)$$

and

$$M(r) = 4\pi \int_0^r \epsilon(r') r'^2 dr'. \quad (14)$$

The above equations describe the structure of a static, spherical and isotropic star with the pressure  $p(r)$  and the energy density  $\epsilon(r)$  reflecting the underlying nuclear model;  $M(r)$  denotes the mass inside a sphere of radius  $r$ . The TOV equations

involve various constraints and boundary conditions: they must be evaluated for the initial condition  $\epsilon(0) = \epsilon_c$  (with  $\epsilon_c$  denoting the central density) and  $M(0) = 0$  at  $r = 0$ ; the radius  $R$  of the star is determined under the condition that on its surface the pressure vanishes,  $p(r)|_{r=R} = 0$ .

The condition for chemical equilibrium for protoneutron stars are:

$$\mu_i = b_i \mu_n - q_i (\mu_\ell - \mu_{\nu_\ell}) \quad (15)$$

where  $\mu_i$  and  $\mu_\ell$  stand for the baryon and lepton chemical potentials, respectively;  $b_i$  is the baryon number and the baryon and lepton electrical charges are represented by  $q_i$ .

The corresponding equations for baryon number and electric charge conservation are:

$$\rho_{baryonic} = \sum_B \frac{k_{F,B}^3}{3\pi^2}, \quad (16)$$

and

$$\sum_B q_{e,B} \frac{k_{F,B}^3}{3\pi^2} - \sum_\ell \frac{k_{F,\ell}^3}{3\pi^2} = 0. \quad (17)$$

In the figures below, the bulk properties of the protoneutron star as a function of the temperature are shown. Figs.9 and 10 show respectively the maximum mass and its radius for hyperon matter including neutrino trapping (solid curve) and the inverse situation, where neutrinos escape freely (dotted curve). These curves indicate maximum masses respectively equal to  $M_{lim} = 1.547M_\odot$  for the former case and  $M_{lim} = 1.557M_\odot$  for the latter. Inspection of these figures indicates that for temperatures higher than 70 MeV equilibrium is obtained for lower masses and radii. If  $T < 70$  MeV the limiting mass increases with temperature.

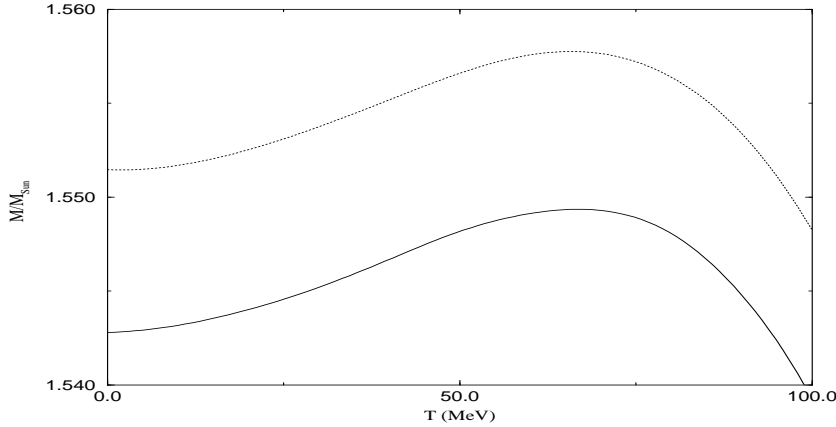


Figure 9: Protoneutron star maximum mass as a function of temperature for  $Y_l = 0.4$  (solid line) and  $Y_L = 0$  (dotted line).

The analysis of the maximum mass vs. temperature relationship is not trivial because of the complex structure of the TOV equations and those describing the thermodynamical state of matter. In one hand, to the increase of temperature it corresponds an increase of the mass of the protoneutron stars, a very well known result for the model used in this calculation<sup>8</sup>; however, other models predict exactly the opposite behaviour. The novel feature we have found without any doubt is an absolute limiting value for the protoneutron star mass, followed by a subsequent

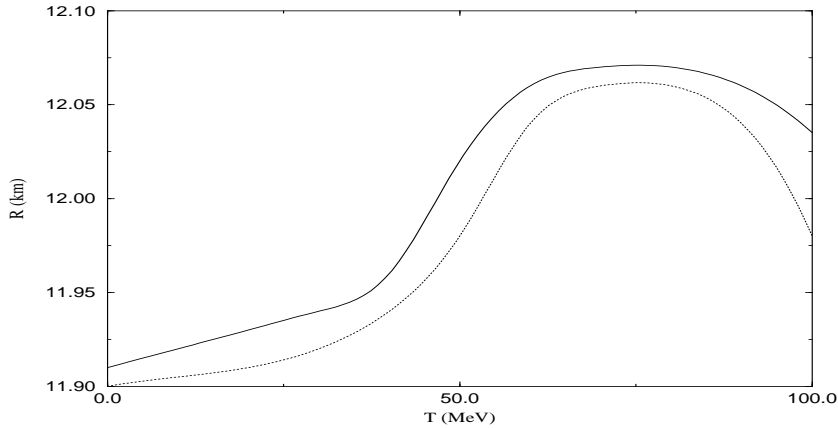


Figure 10: Radii of protoneutron stars with maximum-mass as a function of temperature for trapped (solid line) and for free (dotted line) neutrino matter, respectively.

decrease of this maximum value with the increasing of temperature. The existence of this maximum mass for protoneutron stars, reached at  $T \sim 70 \text{ MeV}$  is a new result obtained in this study and we mention initially three possible reasons to explain it: the very sensible balance of pressure, energy density and gravity in the TOV equations; the modification of the lower limit on the energy density determined by thermal contributions, and the complex behaviour of the scalar field at finite temperature. Here we briefly comment on the last two aspects and in the following we present some analytical estimates for this behaviour.

As temperature increases, due to thermal contributions, an increasingly minimal value for the energy density of nuclear matter is progressively reached. Our results indicate that, when taking into account into the calculations this characteristic behaviour of the thermal energy density, it implies sharper crusts for  $T > 0$ , as compared to the corresponding results at zero temperature. As this effect starts to be significant around  $T = 50 \text{ MeV}$ , it might be a signal that the maximum protoneutron star mass starts to decrease.

A more microscopic and most interesting explanation for the results previously stressed, with striking consequences for nuclear matter at high densities, can be found in the opposite behaviour of the meson scalar field at the high and low density regimes. At low baryon densities, the scalar field does not change significantly as a function of temperature until  $T$  reaches several tens of MeV; then, from this value on, it starts to increase. On the contrary, for high baryon densities, the scalar meson field decreases as the temperature increases already beyond the first few MeV. As the temperature increases, this behaviour becomes even more significant and thus might be basically responsible for the protoneutron star maximum mass behaviour exhibited here.

The temperature dependence of the maximum star mass is supported by analytical estimates of the  $T$ -dependence of the compression modulus and the equation of state of nuclear matter.

Concerning the compression modulus of nuclear matter,

$$K(\rho_0, T) = 9\rho_0^2 \left[ \frac{dp}{d\rho} \Big|_{\rho=\rho_0} \right]$$

$$= 9\rho_0^2 \left[ \frac{\partial p}{\partial \rho} \Big|_{\rho=\rho_0} + \frac{\partial p}{\partial T} \left( \frac{\partial \rho}{\partial T} \right)^{-1} \Big|_{\rho=\rho_0} \right], \quad (18)$$

we find for its leading dependence in T

$$K(\rho_0, T) = K(\rho_0, T = 0) (1 + aT^2), \quad (19)$$

with  $a = 0.0181$ . This expression indicates that as temperature increases, the compression modulus of the protonneutron star matter also increases, giving a stiffer equation of state, for a fixed density, in comparison to the case  $T = 0$ , with the immediate consequence that the stiffer the equation of state, the more massive becomes the limiting star mass of a family of compact stars.

A second analytical argument involves the threshold equation for a given species of hadrons

$$g_B \mu_n - q_{e,B} \mu_e \geq g_{\omega B} \omega_0 + g_{\rho B} \rho_{03} I_{3B} + (M_B - g_{\sigma B} \sigma), \quad (20)$$

where the isospin term  $g_{\rho B} \rho_{03} I_{3B}$  in the eigenvalue determines whether a species is isospin-favored or unfavored. By using for the chemical potential<sup>16</sup>

$$\mu_B \sim \mu_B(T=0) \left[ 1 - \frac{1}{3} \left( \frac{\pi \kappa T}{2\mu_B(T=0)} \right)^2 \right], \quad (21)$$

with

$$\mu_B(T=0) = g_{\omega B} \omega_0 + g_{\rho B} \rho_{03} I_{3B} + \sqrt{k_B^2 + (M_B - g_{\sigma B} \sigma)^2}; \quad (22)$$

one finds (see also figures (3)-(5)), that at densities relevant for neutron stars the relative density distribution of the hyperons, which contribute to the softening of the equation of state and thus to a reduction of the limiting star mass, is shifted to higher values with increasing temperature. As a consequence, the limiting mass of the protonneutron star will increase in the comparison with the corresponding value at  $T = 0$ . Similar arguments were recently used by Prakash<sup>8</sup> in his studies on compact stars a finite T.

Apart from these considerations, a more complete analysis should involve both TOV equations which allow, for an appropriate discussion, only numerical solutions. On the other hand, still some insights may be obtained from the T-dependence of the energy density  $\epsilon(\kappa, T)$ . Taking the Fourier transform at finite temperature,

$$\begin{aligned} \epsilon(r, T) &= \frac{1}{(2\pi)^{3/2}} \int \epsilon(\kappa, T) e^{i\kappa \cdot r} d^3\kappa \\ &= \frac{1}{(2\pi)^{3/2}} \int_0^\infty d\kappa \kappa^2 \epsilon(\kappa, T) \int_0^\pi e^{i\kappa r \cos(\theta)} \sin(\theta) d\theta \int_0^{2\pi} d\phi \\ &= \frac{4\pi}{(2\pi)^{3/2}} \int_0^\infty d\kappa \kappa^2 j_0(\kappa r) \epsilon(\kappa, T). \end{aligned} \quad (23)$$

and combining this expression with equation (14), we find the following equation for the protonneutron star mass

$$M = \frac{4\pi R}{(2\pi)^{3/2}} \int_0^\infty d\kappa \epsilon(\kappa, T=0) j_1(\kappa R) + \frac{4\pi R}{(2\pi)^{3/2}} \int_0^\infty d\kappa \epsilon_S(\kappa, T) j_1(\kappa R). \quad (24)$$

Above,  $R$  represents the protoneutron star radius and  $\kappa$  is the Fermi momentum; furthermore,  $j_i(\kappa R)$  with  $i = 0, 1$  represent Bessel functions of  $i$ -kind while  $\epsilon_S(\kappa, T)$  denotes the temperature corrections described in the appendix

$$\begin{aligned} \epsilon_S(\kappa, T) &= \sum_{i=B} \frac{\gamma}{12} (k_B T)^2 \left[ 2k_{F,i} E_{F,i} + \frac{k_{F,i}^3}{E_{F,i}} \right] \\ &+ \frac{\gamma}{720} \pi^2 (k_B T)^4 \left[ 12 \frac{k_{F,i}}{E_{F,i}} - 9 \left( \frac{k_{F,i}}{E_{F,i}} \right)^3 + 3 \left( \frac{k_{F,i}}{E_{F,i}} \right)^5 \right], \end{aligned} \quad (25)$$

with  $k_{F,B} = \kappa$  (see equation (A.5)). Evidently, one identifies the first term in expression (24) as the protoneutron star mass at  $T=0$  and the second term as finite temperature corrections; the Bessel function in expression (24) modulates the kernel of the integral. As a crucial point, from the spectrum of the energy density, low momenta  $\kappa$  (with  $\kappa R$  below the first zero of the Bessel function) dominate the integration over  $\kappa$  and add up coherently, resulting in an increase of the protoneutron star mass as a function of  $T$ .

We remark that our conjecture is supported both by a quite similar result in the non-relativistic limit obtained by Chandrasekhar<sup>14</sup> in the description of the so called Chandrasekhar mass (see also Baron and Cooperstein<sup>15</sup>) and from the studies recently performed by Woosley and Weaver on the birth of neutron stars<sup>16</sup>, who find for the temperature correction in the protoneutron star mass

$$M \approx M_{T=0} \left( 1 + \frac{\pi^2 \kappa^2 T^2}{\epsilon_F^2} \right) \quad (26)$$

with  $\epsilon_F$  being the Fermi energy.

The inclusion of quarks has a significant impact on the maximum mass of a neutron star: hybrid stars may develop a QGP core, which may extend several kilometers, lowering its maximum mass due to the stiffening of the EOS. For this reason, to develop a treatment compatible with the increasing of this value, we have adopted here different parameterizations for the nuclear matter equation of state. At even higher central densities one can find other classes of stars, for instance strange and quark stars, which are basically formed by deconfined quark matter with a thin (1 km) crust of nuclear matter.

However, there is a very important condition which shall be taken into account when phase transitions are considered in neutron stars. The Seidov criterium<sup>17</sup> establishes that whenever a density or/and an energy density jump exists inside the star, consequence of a phase transition of any type, the resulting configuration is stable only if satisfies the condition

$$\frac{\epsilon_2}{\epsilon_1} < \frac{3}{2} \left( 1 + \frac{p}{\epsilon_1} \right), \quad (27)$$

where  $p$  is the pressure at the interface between both phases, while  $\epsilon_2$  and  $\epsilon_1$  are respectively the energy densities for the higher and lower density phases. It should be emphasized that this criterium is applicable for fully relativistic star models.

The models described in this work generate hybrid proto-neutron stars which satisfy that condition at zero temperature. However, objects hotter than 20 MeV are not able to satisfy the Seidov criterium and become unstable as soon as they underwent a phase transition.

## 5. Summary and Conclusions

In the framework of the Sommerfeld approximation, we have studied the structure of protoneutron stars through an effective many-body field theory at finite temperature. To the best of our knowledge, the approach used in this work, including the Seidov criterium, was followed for the first time in the present investigation of this topic. The Sommerfeld approximation permits a drastic simplification of the computational input and thus provides a rather clear insight in the role of temperature on bulk static properties of these fascinating stellar objects.

The calculations were performed by using an extended version of the non-linear BB model, including the fundamental baryon octet,  $\sigma$ ,  $\omega$  and  $\rho$  mesons, leptons degrees of freedom, trapped neutrinos, — introduced into the formalism at fixed lepton fractions, — the equations for chemical equilibrium and charge neutrality. Integrating the TOV equations we have obtained the maximum mass and the corresponding radius of the protoneutron star as functions of the temperature.

The results indicate that to the increasing of temperature, it corresponds the increasing of the maximum mass and radius of the star and, moreover, that the EOS of nuclear matter becomes stiffer. The causal limit is exactly recovered in the EOS, even in the Sommerfeld approximation, where its recovering becomes more transparent. However, at very high temperatures, the EOS acquires, compared to the  $T = 0$  results, a lower limit on the energy density which prevents the increasing of the maximum mass of the protoneutron star; beyond a critical temperature, which we have found equal to  $T = 70\text{MeV}$ , the maximum mass of protoneutron stars decreases.

We have analyzed the protoneutron star structure with and without neutrino trapping and the corresponding maximum masses obtained are  $1.557 M_\odot$  and  $1.547 M_\odot$ , respectively, for the set of parameters shown in table 1. We have identified this value as the maximum protoneutron star mass which can be formed right after the supernova event. With the same parameters in table 1, except for the choice of the hyperon-nucleon coupling ratios<sup>4</sup>  $\chi_\sigma = \chi_\omega = \chi_\rho = \sqrt{2/3}$ , we have obtained respectively  $1.889 M_\odot$  and  $1.868 M_\odot$ . These last values are able to explain the mass of the neutron star in the binary system Vela X-1<sup>5</sup> and this example illustrates how these mass determinations may guide us in the choice of adequate nuclear interaction coupling constants.

In figure 11 we exhibit the behaviour of the protoneutron star mass as the temperature increases (in order to group three different stars in the same plot, we normalize the protoneutron star masses by their values at zero temperature). Each of the three sets of stars are chosen to have the same total baryon number.

We also have seen that a hybrid protoneutron star, which shall obey the Seidov criterium, can only be formed at low temperatures of the order of  $T=20\text{MeV}$ . Protoneutron stars hotter than that value shall first cool down as hyperon stars and may form, subsequently, a quark core in its inner region.

The density dependence of the scalar meson field is of particular interest for dense hadronic systems in general, as it touches upon the basic question how to organize effective field theories. Here two scenarios are obvious, which lead to a drastically different dependence of the nonlinear scalar (and vector) meson field with density and temperature. In the naive dimensional analysis, the scale parameter for natural nonlinear self-coupling of the  $\sigma$  and  $\omega$  fields is the effective mass scale

$$m_{eff} \sim \sqrt{f_\pi \Lambda} \sim (250 - 300\text{MeV}),$$

at saturation density, with  $f_\pi \sim 93\text{MeV}$  as the weak  $\pi$ -decay constant and  $\Lambda \sim$  nucleon mass as the scale for chiral symmetry breaking. From arguments based on Brown-Rho scaling and the onset of deconfinement with the appearance of a quark-gluon plasma beyond some critical density  $\rho_c \sim 4\rho_0$ , both  $f_\pi$  and  $\Lambda$  and thus  $m_{eff}$  decreases with increasing  $\rho$  yielding

$$m_{eff} \sim 0 \text{ for } \rho > \rho_c.$$

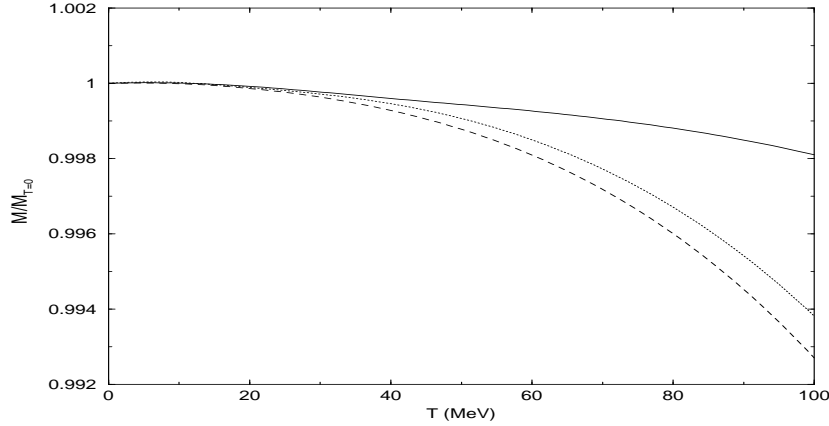


Figure 11: Protoneutron star mass normalized by its mass at  $T=0$ , as function of temperature for  $M_{T=0} = 1.8M_{\odot}$  (solid line),  $M_{T=0} = 1.6M_{\odot}$  (dotted line) and  $M_{T=0} = 1.35M_{\odot}$  (dashed line).

Thus organizing effective field theory with the scale mass  $\sqrt{f_{\pi}\Lambda}$  would completely change the role of high order meson self-couplings — in the limit  $m_{eff} \rightarrow 0$  the corresponding lagrangian would develop an essential singularity — and at the same time, used as a scale parameter for the temperature dependence

$$\lambda \sim \frac{\kappa T}{m_{eff}},$$

would invalidate the Sommerfeld approximation beyond a critical density.

However, an alternative scale for fermionic matter is set by the Fermi-momentum  $k_F$  itself. At saturation density the two scales coincide: at  $\rho = \rho_0$

$$m_{eff} \sim \sqrt{f_{\pi}\Lambda} \sim k_F \sim 270 \text{ MeV}.$$

Opposite to  $m_{eff}$ , however,  $k_F$  is stable, as it increases typically as  $k_F \sim \rho^{1/3}$  with increasing density. Such an organizational scheme of effective field theory would preserve both the dominance of the cubic and quartic  $\sigma$  (and  $\omega$ ) self-couplings and with the expansion parameter

$$\lambda \sim \frac{\kappa T}{k_F} \sim \frac{\kappa T}{(270 \text{ MeV})(\rho/\rho_0)^{1/3}},$$

would even improve the convergence of the Sommerfeld approximation with increasing density.

Our investigations are just a first attempt towards the comprehension of the role of temperature on physical properties of neutron stars. Our main findings are substantiated by calculations based on improved microscopic models, which include as an example, in the spirit of the Brown-Rho scaling, a density dependence of the coupling constants in the model. Investigations along these lines are in progress.

## Appendix A

The finite temperature studies involves many technical difficulties through the Fermi integrals; in particular, the computational effort increases dramatically. However, as from the integration of the full energy density only a narrow range contributes significantly to observables, approximate schemes should provide at least

semi-quantitative results. The Sommerfeld approximation is a very successful approach first applied in condensed matter physics and recently applied to the white dwarf problem<sup>18</sup>. We briefly describe, in this section, the Sommerfeld approximation and discuss its validity when applied to nuclear matter problems. The main conception of the approximation is the following: if a given function  $H(\epsilon)$  of the energy density  $\epsilon$  does not vary rapidly in the energy range of the order of  $\kappa T$  around  $\mu$ , the temperature dependence of the integral  $\int_{-\infty}^{\infty} H(\epsilon)n(\epsilon)d\epsilon$  should be given quite accurately by replacing  $H(\epsilon)$  by the first few terms in its Taylor expansion around  $\epsilon = \mu$ :

$$H(\epsilon) = \sum_{n=0}^{\infty} \frac{d^n}{d\epsilon^n} H(\epsilon) \Big|_{\epsilon=\mu} \frac{(\epsilon - \mu)^n}{n}. \quad (\text{A.1})$$

The result is a series of the form

$$\int_{-\infty}^{\infty} H(\epsilon)n(\epsilon)d\epsilon = \int_{-\infty}^{\mu} H(\epsilon)d\epsilon + \sum_{n=1}^{\infty} (\kappa T)^{2n} a_n \frac{d^{2n-1}}{d\epsilon^{2n-1}} H(\epsilon) \Big|_{\epsilon=\mu}. \quad (\text{A.2})$$

The coefficients  $a_n$  are dimensionless constants of order  $\mathcal{O}(1)$ , and are determined according to

$$a_n = \int_{-\infty}^{\infty} \frac{x^{2n}}{(2n)} \left( -\frac{d}{dx} \frac{1}{e^x + 1} \right) dx. \quad (\text{A.3})$$

The functions  $H(\epsilon)$  of our approach have major variations on energy scales of the order of  $\mu$  and thus in general  $(d/d\epsilon)^n H(\epsilon)|_{\epsilon=\mu}$  is of the order of  $H(\mu)/\mu^n$ . Consequently, successive terms in the Sommerfeld approximation are smaller by  $\mathcal{O}((\kappa T)^2) \sim \mathcal{O}(10^{-4})$ . Consequently, in actual calculations only the first few terms must be retained. The final form of the integrals, up to the third order, is then given as

$$\begin{aligned} \int_{-\infty}^{\infty} H(\epsilon)f(\epsilon)d\epsilon &= \int_{-\infty}^{\mu} H(\epsilon)d\epsilon + \frac{\pi^2}{6}(\kappa T)^2 H'(\mu) \\ &+ \frac{7\pi^4}{360}(\kappa T)^4 H'''(\mu) + \mathcal{O}\left(\frac{\kappa T}{\mu}\right)^6, \end{aligned} \quad (\text{A.4})$$

where we recognize the zero temperature contribution corrected by terms which include explicitly the temperature.

We describe, in the following, the EOS of nuclear matter at finite temperature, extending the  $T = 0$  energy density  $\epsilon_0$  and pressure  $p_0$ , by the leading  $T$ -dependent coefficients from the Sommerfeld approximation:

$$\begin{aligned} \epsilon &= \epsilon_0 + \sum_{i=B,\ell} \frac{\gamma}{12} (k_B T)^2 \left[ 2k_{F,i} E_{F,i} + \frac{E_{F,i}^3}{k_{F,i}} \right] \\ &+ \frac{\gamma}{720} \pi^2 (k_B T)^4 \left[ 12 \frac{E_{F,i}}{k_{F,i}} - 9 \left( \frac{E_{F,i}}{k_{F,i}} \right)^3 + 3 \left( \frac{E_{F,i}}{k_{F,i}} \right)^5 \right]; \end{aligned} \quad (\text{A.5})$$

$$\begin{aligned} p &= p_0 + \sum_{i=B,\ell} \frac{\gamma}{12} (k_B T)^2 \left[ \frac{4E_{F,i}^3}{k_{F,i}} - \frac{E_{F,i}^5}{k_{F,i}^3} \right] \\ &+ \frac{\gamma}{720} \pi^2 (k_B T)^4 \left[ 24 \frac{E_{F,i}}{k_{F,i}} - 39 \left( \frac{E_{F,i}}{k_{F,i}} \right)^3 + 9 \left( \frac{E_{F,i}}{k_{F,i}} \right)^5 + 15 \left( \frac{E_{F,i}}{k_{F,i}} \right)^7 \right]. \end{aligned} \quad (\text{A.6})$$



In previous appreciations, the Sommerfeld approximation has been used to describe systems in the high density and low temperature ranges,  $\frac{\mu}{k_B T} \gg 1$ , a condition which is very well satisfied in protoneutron stars, with typically  $\frac{\mu}{k_B T} \sim [10 - 10^2]$ ; with this in mind, we feel confident about the adequacy of the approach for the investigation here exhibited. However, to explore quantitatively the limiting range of validity of the Sommerfeld approximation, we have performed calculations for less complex microscopic models and compared the approximate results with numerically rigorous calculations (see figure (A.1)).

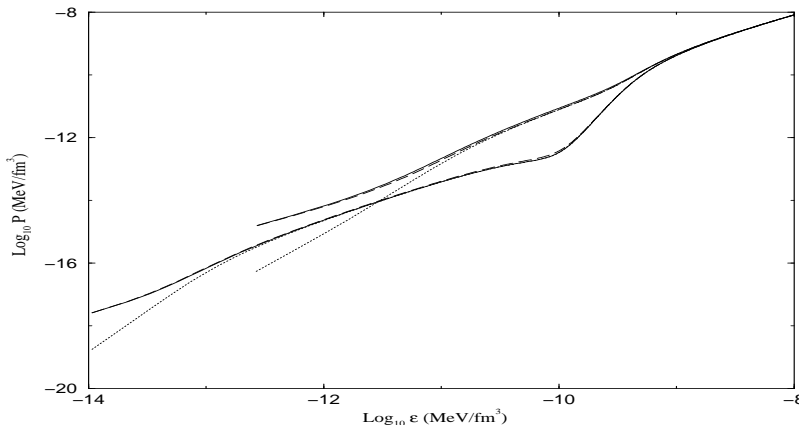


Figure A.1: EOS for the Walecka model for the temperatures  $T = 50$  MeV and  $10$  MeV (upper and lower curves, respectively). Solid lines: exact results; dashed and dotted lines: first and second order corrections of the Sommerfeld approximation.

We have used, in particular, the Sommerfeld approximation to describe the equation of state of the original QHD model for pure neutron matter. Then, the equation of state was combined with the TOV equations, giving the results shown in table A.1 for the exact calculations and the approximated ones using the Sommerfeld based calculations. We have tested our results at the critical temperature for the liquid-gas phase transition in nuclear matter ( $T=9.2$ MeV) and for higher values ( $T=50$ MeV), as typically found in protoneutron stars. For comparison, the maximum mass predicted in the Walecka model at  $T = 0$  is  $2.57M_{\odot}$ .

Temperature	Exact	Sommerfeld
9.2MeV	2.606	2.605
50MeV	3.215	3.144

Table A.1: Comparative results of the maximum protoneutron star mass.

The (nearly) quantitative results of the two approaches confirms the adequacy of the utilization of the Sommerfeld approximation in the description of physical properties of nuclear matter at finite temperature.

### Acknowledgements

This work was funded by CAPES and CNPq. The authors wish to thank Prof. M.A.C. Gusmão for helpful discussions.

1. A. Hewish, S. J. Bell, J. D. H. Pilkington, P. F. Scott and R. A. Collins, *Nature* **217**, 709 (1968).

2. R. C. Tolman, *Phys. Rev.* **55**, 364, (1939).
3. J. R. Oppenheimer and G. M. Volkoff, *Phys. Rev.* **55**, 374, (1939).
4. N. K. Glendenning, *Compact Stars* (Springer-Verlag, 1997).
5. O. Barziv, L. Kaper, M.H. van Kerkwijk, J.H. Telting, J. van Paradijs, astro-ph/0108237.
6. J. D. Walecka and B. D. Serot, *Advances in Nuclear Physics* **16** (Plenum Press, 1986).
7. J. Boguta and A. R. Bodmer, *Nucl. Phys.* **A292**, 413, (1977).
8. M. Prakash, I. Bombaci, M. Prakash, P. J. Ellis, J. M. Lattimer, J. M. and R. Korren, *Phys. Rep.* **280**, 1, (1997).
9. N. K. Glendenning, F. Weber, S. A. Moszkowski, *Phys. Rev.* **C45**, 844, (1992).
10. W. Koepf, M. M. Sharma and P. Ring, *Nucl. Phys.* **A533**, 95, (1992).
11. A. Chodos, R. L. Jaffe, K. Johnson, C. B. Thorn and V. F. Weisskopf, *Phys. Rev.* **D9**, 3471, (1974).
12. T. de Grand, R. L. Jaffe, K. Johnson, J. Kiskis, *Phys. Rev.* **D12**, 2060, (1975).
13. L. Landau and E. Lifchitz, *Mécanique Statistique* (Éditions Mir, 1967).
14. S. Chandrasekhar, *An Introduction to the Study of Stellar Structure* (University of Chicago Press, 1939).
15. E. Baron and J. Cooperstein, *Ap. J.*, **132**, 597 (1990).
16. S. E. Woosley and T. A. Weaver, *The Structure and Evolution of Neutron Stars: conference proceedings* (Addison-Wesley Publishing Company, 1992)
17. Z. F. Seidov, *Astron. Zh.* **48**, 443, (1971).
18. G. Bertone and R. Ruffini, to appear in the *Proceedings of Marcel Grossmann IX*, (World Scientific), astro-ph/0105143.
19. S. Weinberg, *Gravitation and Cosmology* (John Wiley, 1972).